Regularization of Diffusion MRI Q-Ball Fields for Crossing Fiber Tractography

K.M. Otto[1], H.H. Ehricke[1], V. Kumar[2] and U. Klose[2]

[1] Institute for Applied Computer Science, University of Applied Sciences, Stralsund, Germany
[2] Section of Experimental NMR of the CNS, University Hospitals, Tübingen, Germany

Abstract— **Since the advent of high angular resolution diffusion imaging (HARDI) techniques in diffusion MRI great efforts have been taken in order to reconstruct complex white-matter structures, such as crossing, branching and kissing fibers. However, even highly sophisticated fiber tracking schemes, such as probabilistic tracking, suffer from the data's poor signal-to-noise (SNR) ratio. In this paper we present a novel regularization approach for q-ball fields, exploiting structural information within the data. We also propose a straightforward deterministic tracking algorithm, allowing delineation of even non-dominant pathways through crossing regions. Results from a phantom study with a biological phantom as well as a patient study, in which we reconstruct a part of the pyramidal tract, emphasize the method's efficiency.**

Keywords— **HARDI, ODF, Regularization, Fiber Tracking**

I. Introduction

In Magnetic Resonance Diffusion Imaging the diffusion tensor has been widely used as a model for the diffusion behaviour of water molecules in a voxel. However, for the delineation of more complex structures, such as kissing, crossing or branching fibers, high angular resolution diffusion imaging (HARDI) techniques which rely on the acquisition of far more than 60 gradient directions have emerged. Unfortunately, these methods are highly susceptible to artifacts, e.g. resulting from eddy currents or motion shift, and especially to noise.

A common way of describing diffusion in a voxel is the Orientation Distribution Function (ODF) which can be reconstructed in a model-independent manner known as Q-Ball Imaging (QBI) [1]. An ODF for a voxel at a discrete position (x_i, y_i, z_i) in 3D space may be imagined as a projection of diffusion probabilities p_{ij} onto the surface of a unit sphere, constructed around that voxel. Each diffusion probability p_{ij} corresponds to a discrete reconstruction point r_j on the unit sphere surface. For each of the reconstructed surface points r_j, its ODF value p_{ij} describes the diffusion probability in the direction $\mathbf{r}_j$ given by the unit vector from the sphere's centre to the surface point. Thus we can describe an ODF as a discrete functional

$$\Psi_i(r_j) = p_{ij} \qquad (1)$$

Due to symmetry reasons it is enough to distribute the datapoints r_j on a half-sphere.

The sphere-shaped ODF can be radially distorted based upon the probability values p_{ij}, leading to a geometric representation of the spatial diffusion profile. Rescaling to the minimum to maximum interval of diffusion probabilities enhances the sharpness of that shape. Local smoothing, e.g. using a spherical Gaussian kernel, can be applied in order to address the ODF's low signal-to-noise ratio (SNR). However, this may suppress important details, e.g. signals stemming from non-dominant fibers.

During the last five years a variety of authors have proposed novel HARDI-based approaches, both multiple-orientation deterministic methods as well as highly sophisticated and computationally expensive probabilistic techniques [2][3][4][5]. Most of them could improve the results for the delineation of specific brain regions with more complex white matter populations. Nevertheless, we are far from a general, clinically applicable solution.

II. Diffusion MRI Regularization

In diffusion MRI the last decade has seen various approaches, most of them focused on diffusion tensor regularization. They fall into three categories, namely

1. regularization of diffusion weighted images, prior to tensor reconstruction [6][7],
2. incorporation of a regularization scheme into the tensor estimation process [8],
3. regularization of tensor fields [9][10].

Only a few novel techniques have been proposed for ODF regularization. Savadjiev et al. [11] model fibers by chains of helical segments. They use the notion of co-helicity in order to compute confidence values of ODF-directions of neighboring voxels providing an estimate of local support. The drawbacks are computational expensiveness and the method's high complexity, making the interpretation of unwanted effects not easy. Jonasson et al. [12] use ODF regularization, prior to the segmentation of major white-matter tracts. Within a five-dimensional position-orientation space (POS) they perform anisotropic diffusion filtering in order to produce multiple scales of resolution for the data. However, the spatial resolution and

ODF sharpness is reduced with increasing degree of regularization. Descoteaux et al. [13] use spherical harmonics for ODF reconstruction. They incorporate a Laplace-Beltrami operator into the reconstruction scheme which reduces the influence of higher-order terms due to noise. Moreover they propose to transform the relatively unsharp and noisy Diffusion-ODF into a sharper Fiber-ODF by deconvolution with a diffusion-ODF kernel of a linear fiber model [14].

III. ODF REGULARIZATION BY CONE-BEAMS

By restricting ODF smoothing to the data, available within a voxel, we usually loose angular resolution or limit the regularization effect. Another way, commonly used in image processing, is to incorporate information from neighboring voxels into the process. In the case of ODF de-noising our goal is to design a filter scheme, allowing smoothing along fiber trajectories only. Thus, we use structural information, given by the ODF functional, in order to avoid smoothing over anisotropic regions with different diffusion orientations. In our cone-beam regularization (CB-REG) approach we apply smoothing to each datapoint p_{ij} on the ODF sphere at position (x_i, y_i, z_i) in 3D space. The datapoint's local neighborhood is defined by its direction vector $\mathbf{r}_j$ and two parameters α and l, describing opening angle and length of the cone-shaped neighborhood. The cone is centered around the direction vector $\mathbf{r}_j$ (cone A). Since the ODF is a symmetric function, a second cone B is constructed in the opposite direction $-\mathbf{r}_j$. Within each cone rays are sent along all direction vectors $\mathbf{r}_k$ encompassed by the cone shape: $\angle(\mathbf{r}_k, \mathbf{r}_j) \leq \alpha/2$ (see fig. 1). Each ray is then sampled by tri-linear interpolation of ODFs at each unit step along the ray until the length of the cone has been reached. From each of the ODFs, sampled along a certain ray, only the single datapoint, whose direction coincides with the ray direction, is relevant. All relevant datapoints p_{mk}, which have been sampled inside the cone, are used in order to compute a smoothed ODF value $\Psi^{\sim}_i(r_j)$ by a weighted sum. We apply a two-dimensional Gaussian kernel $G(d,\delta)$ to scale each datapoint's weight according to its Euclidean distance $d_{mi} = ((x_m-x_i)^2+(y_m-y_i)^2+(z_m-z_i)^2)^{0.5}$ from the cone center and the angle $\delta_{kj} = \angle(\mathbf{r}_k, \mathbf{r}_j)$ between its direction $\mathbf{r}_k$ and the direction $\mathbf{r}_j$ around which the cone is centered. Thus the filtered ODF value $\Psi^{\sim}_i(r_j)$ is derived from the set of sampled ODF values $p_{mk} = \Psi_m(r_k)$ by:

$$\Psi^{\sim}_i(r_j) = \frac{1}{w} \sum_{m\in M, k\in K} G(d_{mi}, \delta_{kj}) \Psi_m(r_k) \qquad (2)$$

where

M: set of sampled positions within cone A and B

K: set of sampled ray directions within cone A and B

w: sum of all weights of the sampled datapoints within cone A and B:

$$w = \sum_{m\in M, k\in K} G(d_{mi}, \delta_{kj}) \qquad (3)$$

and

$$G(d,\delta) = e^{-\frac{d^2}{\sigma_d^2} - \frac{\delta^2}{\sigma_\delta^2}} \qquad (4)$$

The parameters σ_d and σ_δ define the sharpness of the two-dimensional Gaussian kernel. For simplification, we define a weight ω for the farthest distance $d = l$ and the widest angle $\delta = \alpha/2$ and compute σ_d and σ_δ such, that the utmost sample reaches a weight of ω.

In this manner we smooth only over a neighborhood of equal or similar diffusion directions, thus exploiting the structural information, given by the ODF itself.

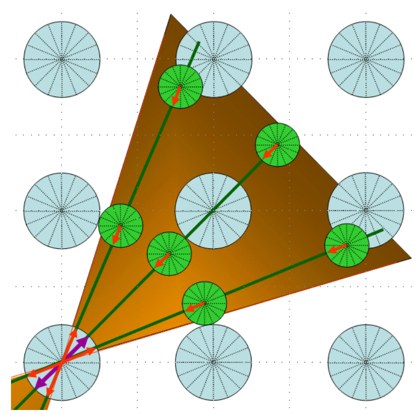

Fig. 1 Sketch of neighborhood sampling strategy used in cone-beam regularization, illustrating cone construction and sampling for a single ODF datapoint. Around the datapoint's direction and opposite direction (bold arrows) two cones are constructed. Within each cone ODFs are sampled (small circles) along direction rays by tri-linear interpolation within the ODF field (big circles). Only datapoints with directions along sampling rays are accepted (thin red arrows).

IV. TRACKING THROUGH Q-BALL FIELDS

There has been a broad range of publications about fiber tractography algorithms, both deterministic and probabilistic. While deterministic methods, such as streamline tracking [15] or tensor deflection (TEND) [16], benefit from simplicity and computational efficiency, more sophisticated deterministic and especially probabilistic methods have been elaborated [2][17][3][18][19] in order to

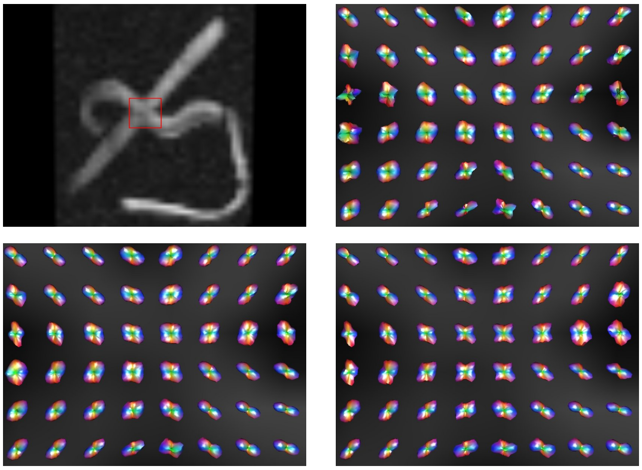

Fig. 2 Slice through phantom GFA data (top left) and ODFs in crossing area before (upper right) and after regularization with different parameters (lower row).

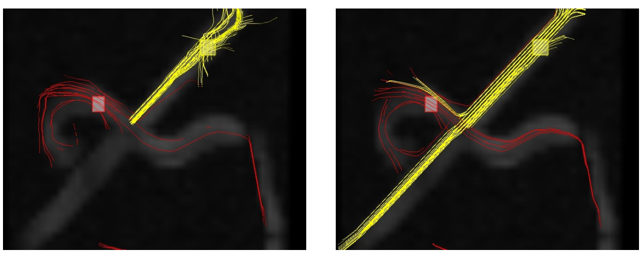

Fig. 3 Tracking result from phantom study with two seed boxes using original ODFs (left) and after regularization (right).

address uncertainty, noise artifacts and partial voluming effects in regions of complex white matter structure.

Since we want to study the impact of our regularization approach on fiber tractography, we use a simple and straightforward deterministic algorithm which does not rely on a complex model and can easily be parameterized. From a seed voxel we start in the direction of the ODF's global maximum. At each integration step, we construct a cone around the incident direction. If this cone contains a direction, whose probability is at least 80 percent of the ODF's global maximum, we proceed in that direction. Otherwise, we stop tracking because there is obviously no indication to move further in any of the directions enclosed by the cone. In our experiments, we used a tracking step width of 0.25 voxels, a cone opening angle of 40° and a minimum anisotropy (GFA) value of 0.3. Though such a tracking scheme is rather simple, it allows tracking fibers through crossing regions, without being deflected by major pathways. Of course, the latter can only be achieved, if the ODFs in the q-ball field are sharp enough and their SNR is sufficiently high. But this is exactly what our regularization approach aims at.

V. Results

For the evaluation of our regularization approach diffusion phantom data, provided by McGill University, Toronto was used. The phantom was constructed from excised rat spinal cord, embedded in agar in a configuration designed to have curved, straight and crossing tracts [20] (fig. 2). The q-ball data was acquired on a 1.5 Tesla Sonata MR scanner (Siemens, Erlangen) with 90 diffusion weighting directions, 30 slices and an isotropic resolution of 2.8 mm.

Fig. 2 shows the generalized fractional anisotropy (GFA) values from a slice through the phantom dataset (top left). The original ODFs are illustrated by the zoomed ODF shape display of the crossing region (top right). In the lower row results from ODF regularization with different parameters are displayed. In the left picture a cone length l of 2 voxels was used, whereas the right picture was produced with $l = 4$ voxels. In both cases a cone opening angle α of 30° and a ω of 0.5 were used. The results illustrate, that the regularization sharpens the ODFs and that with increasing cone length the effect becomes more obvious. The regularized ODFs within the fiber crossing area clearly show the expected bi-directional anisotropic behavior.

We also applied the tracking algorithm, described above to the regularized as well as the original phantom data. Fig. 3 shows the streamlines, which were generated by usage of two seedboxes. Tracking through the crossing region fails due to partial voluming (left picture). After regularization with $\alpha = 30°$, $l = 2$ voxels and $\omega = 0.25$ the results are much better. Note, that smoothing with a relatively small voxel neighborhood is obviously sufficient to substantially enhance tracking results.

Furthermore, we applied our method to data from a patient study, acquired on a 3 Tesla Trio scanner (Siemens, Erlangen) with an isotropic resolution of 2.0 mm, 126 gradient directions and 56 slices. Each 10 diffusion measurements were followed by a non-diffusion measurement, which was used to estimate the rotation matrices of a head motion correction procedure. Furthermore, an eddy current correction was performed. We focused on the delineation of the pyramidal tract. Many studies have shown, that especially near the corpus callosum tracking of pyramidal fibers is difficult because of crossing callosal projections. This finding was confirmed by our tracking experiments, using non-regularized q-ball fields (fig. 4, left picture). After regularization with our CB-REG approach, substantially more fibers could be tracked

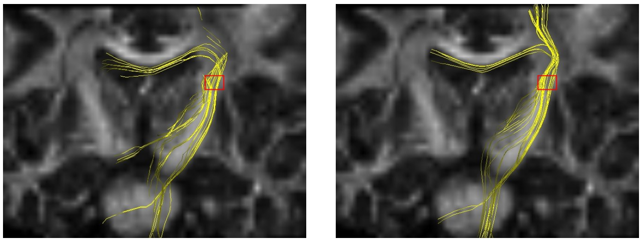

Fig. 4 Tracking result from pyramidal tract with one seed box, using original ODFs (left) and after regularization (right).

through the crossing region (right picture). Again we used a relatively small voxel neighborhood for ODF denoising: $\alpha = 30^{\circ}$, $l = 2$, $\omega = 0.5$.

VI. Conclusions

We have presented a new method for regularization of q-ball fields, which does not depend on highly complex modeling assumptions. We use a cone-beam strategy with 3 parameters to sharpen the ODF's shape and reduce noise. Our experiments show, that tracking fiber pathways through crossing regions benefits from the regularization of the q-ball field. Care has to be taken, not to overdo the regularization effect, e.g. by the definition of an arbitrarily large neighborhood. Artifacts might be induced, constructing wrong connections. Currently we elaborate our strategy by incorporating anisotropy data (GFA values) into the regularization scheme to reduce the erroneous influence of neighboring isotropic voxels on ODFs representing regions at fascicle borders.

Acknowledgment

We would like to thank Jennifer Campbell of the McConnell Brain Imaging Centre, Montreal Neurological Institute, McGill University, for providing the phantom data, we used in our experiments.

References

1. Tuch D S (2004) Q-ball imaging. Magn Reson Med 52:1358–1372
2. Parker G J M, Haroon H A, Wheeler-Kingshott C A M (2003) A framework for a streamline-based probabilistic index of connectivity (PICo) using a structural interpretation of MRI diffusion measurements. J Magn Reson Imaging 18:242–254
3. Lazar M, Alexander A L (2005) Bootstrap white matter tractography (BOOT-TRAC). Neuroimage 24:524–532
4. Behrens T E J, Berg H J, Jbabdi S, Rushworth M F S, Woolrich M W (2007) Probabilistic diffusion tractography with multiple fibre orientations: What can we gain? Neuroimage 34:144–155
5. Zalesky A (2008) DT-MRI fiber tracking: a shortest paths approach. IEEE Trans Med Imaging 27:1458–1471
6. Parker G J, Schnabel J A, Symms M R, Werring D J, Barker G J (2000) Nonlinear smoothing for reduction of systematic and random errors in diffusion tensor imaging. J Magn Reson Imaging 11:702–710
7. Martin-Fernandez M, Muñoz-Moreno E, Cammoun L, Thiran J-P, Westin C-F, Alberola-López C (2009) Sequential anisotropic multichannel Wiener filtering with Rician bias correction applied to 3D regularization of DWI data. Med Image Anal 13:19–35
8. Wang Z, Vemuri B C, Chen Y, Mareci T H (2004) A constrained variational principle for direct estimation and smoothing of the diffusion tensor field from complex DWI. IEEE Trans Med Imaging 23:930–939
9. Poupon C, Clark C A, Frouin V et al. (2000) Regularization of diffusion based direction maps for the tracking of brain white matter fascicles. Neuroimage 12:184–195
10. Coulon O, Alexander D C, Arridge S (2004) Diffusion tensor magnetic resonance image regularization. Med Image Anal 8:47–67
11. Savadjiev P, Campbell J S W, Pike G B, Siddiqi K (2005) 3D curve inference for diffusion MRI regularization. Med Image Comput Comput Assist Interv Int Conf Med Image Comput Comput Assist Interv 8:123–130
12. Jonasson L, Bresson X, Thiran J-P, Wedeen V J, Hagmann P (2007) Representing diffusion MRI in 5-D simplifies regularization and segmentation of white matter tracts. IEEE Trans Med Imaging 26:1547–1554
13. Descoteaux M, Angelino E, Fitzgibbons S, Deriche R (2007) Regularized, fast, and robust analytical Q-ball imaging. Magn Reson Med 58:497–510
14. Descoteaux M, Deriche R, Knösche T R, Anwander A (2009) Deterministic and probabilistic tractography based on complex fibre orientation distributions. IEEE Trans Med Imaging 28:269–286
15. Mori S, Crain B J, Chacko V P, Zijl P C (1999) Three-dimensional tracking of axonal projections in the brain by magnetic resonance imaging. Ann Neurol 45:265–269
16. Lazar M, Weinstein D M, Tsuruda J S et al. (2003) White matter tractography using diffusion tensor deflection. Hum Brain Mapp 18:306–321
17. Behrens T E J, Woolrich M W, Jenkinson M et al. (2003) Characterization and propagation of uncertainty in diffusion-weighted MR imaging. Magn Reson Med 50:1077–1088
18. Ehricke H-H, Klose U, Grodd W (2006) Visualizing MR diffusion tensor fields by dynamic fiber tracking and uncertainty mapping. Computers & Graphics 30:255–264
19. Perrin M, Poupon C, Cointepas Y et al. (2005) Fiber tracking in q-ball fields using regularized particle trajectories. Inf Process Med Imaging 19:52–63
20. Campbell J S W, Siddiqi K, Rymar V V, Sadikot A F, Pike G B (2005) Flow-based fiber tracking with diffusion tensor and q-ball data: validation and comparison to principal diffusion direction techniques. Neuroimage 27:725–736

Author: Kay Michael Otto
Institute: University of Applied Sciences Stralsund,
Institute for Applied Computer Science (IACS)
Street: Zur Schwedenschanze 15
City: Stralsund
Country: Germany
Email: kay.otto@fh-stralsund.de